DoA Estimation Performance and Computational Complexity of Subspace- and Compressed Sensing-based Methods

Christoph Stöckle, Jawad Munir, Amine Mezghani and Josef A. Nossek
Institute for Circuit Theory and Signal Processing
Munich University of Technology, 80290 Munich, Germany
E-Mail: {christoph.stoeckle, jawad.munir, amine.mezghani, josef.a.nossek}@tum.de

***Abstract*—We investigate the Direction of Arrival (DoA) estimation for small- and large-scale antenna arrays with a small and a large number of antenna elements, respectively. Two classes of algorithms are considered, namely subspace- and compressed sensing (CS)-based algorithms. We compare those algorithms in terms of both the DoA estimation performance and the computational complexity based on different parameters such as number of antenna elements, number of snapshots and quantization. From this comparison, we conclude that the subspace-based method ESPRIT is well suited for small-scale antenna systems while the CS-based method IHT is advantageous for large-scale antenna systems.**

I. Introduction

The deployment of very large number of antennas at the base station (BS), also known as massive MIMO, is a potential candidate for the future generation of wireless communication systems. Massive MIMO can increase the spectral efficiency by sending and receiving signals through narrow directed beams [1]. Massive MIMO is defined as a system with M BS antennas and K users, where the inequality $M \gg K$ holds. The massive increase in the number of antenna elements also requires computationally efficient Direction of Arrival (DoA) estimation algorithms. In this paper, we investigate the DoA estimation using subspace- and compressed sensing (CS)-based methods for both small- and large-scale antenna systems with a small and a large number of antenna elements, respectively.

The subspace-based methods such as Multiple Signal Classification (MUSIC) and Estimation of Signal Parameters via Rotational Invariance Techniques (ESPRIT) described in [2] and [3], respectively, use the subspaces of the covariance matrix for the DoA estimation. On the other hand, CS-based methods estimate the DoAs by solving a sparse recovery problem, i.e., reconstructing sparse signals from linear measurements. In CS, the sparse recovery methods like the Basis Pursuit Denoise (BPDN) and the Iterative Hard Thresholding (IHT) algorithm have been developed [4], which can also be used for the DoA estimation. DoA estimation based on CS has already been studied, e.g., in [5] and [6], by formulating it as a sparse recovery problem.

Not only the DoA estimation performance of the methods is important but also their computational complexity. Therefore, we compare the subspace-based methods MUSIC and ESPRIT as well as the CS-based methods BPDN and IHT in terms of both the DoA estimation performance and the computational complexity for small and large-scale antenna arrays. For the subspace-based methods, the eigenvalue decomposition (EVD) of the covariance matrix has to be computed, which leads to a high computational complexity when using large-scale antenna arrays. On the contrary, the computational complexity of IHT might be smaller for large-scale antenna arrays as no EVD is required.

In order to perform DoA estimation on M BS antennas, the received analog baseband signal is converted into the digital domain using analog-to-digital converters (ADCs). It is shown in [7] that the power consumption of the ADCs grows exponentially with the resolution b, i.e., $P_{\text{ADC}} \propto 2^{2b}$. The total ADC power consumed by the M antennas scales linearly with M, i.e., $P_{\text{ADC,tot}} \propto M \cdot 2^{2b}$. The extreme case of a 1-bit ADC is advantageous in terms of power consumption but using only 1-bit resolution generally has a severe impact on the performance. Therefore, it is pertinent to investigate the performance of different algorithms for the special case of 1-bit quantization.

The paper is organized as follows. In section II, a measurement model for the DoA estimation with the help of a Uniform Linear Array (ULA) is introduced. In section III, we describe how the DoAs can be estimated by using the subspace-based methods MUSIC and ESPRIT as well as the CS-based methods BPDN and IHT. Section IV presents the results of the simulations we have conducted in order to examine the DoA estimation performance of the considered methods before the computational complexity of those methods is compared in section V. Finally, section VI concludes the paper.

II. Measurement Model

In this section, a measurement model for the DoA estimation is introduced.

An M-element ULA with an inter-element spacing of half the wavelength is located in the far field of $K < M$ sources emitting narrow-band zero mean signals. It receives the signal $s_k(t) \in \mathbb{C}$ of source $k \in \{1, 2, \ldots, K\}$ from DoA $\theta_k \in [-90°, 90°)$ corresponding to the spatial frequency $\mu_k = -\pi \sin(\theta_k)$. At time instant t, the measurement acquired by the antenna element $m \in \{1, 2, \ldots, M\}$ of the ULA is

ISBN 978-3-8007-3662-1

given by

$$x_m(t) = \sum_{k=1}^{K} s_k(t)\, \mathrm{e}^{j(m-1)\mu_k} + n_m(t), \tag{1}$$

where $n_m(t) \in \mathbb{C}$ is additive measurement noise, which is i.i.d., zero mean and uncorrelated with the source signals.

Using the array steering matrix $\mathbf{A} = [\mathbf{a}(\mu_1), \ldots, \mathbf{a}(\mu_K)] \in \mathbb{C}^{M\times K}$ with $\mathbf{a}(\mu_k) = \left[1, \mathrm{e}^{j\mu_k}, \ldots, \mathrm{e}^{j(M-1)\mu_k}\right]^{\mathrm{T}} \in \mathbb{C}^M$, the signal vector $\mathbf{s}(t) = [s_1(t), \ldots, s_K(t)]^{\mathrm{T}} \in \mathbb{C}^K$ and the noise vector $\mathbf{n}(t) = [n_1(t), \ldots, n_M(t)]^{\mathrm{T}} \in \mathbb{C}^M$, the measurement model for one snapshot or a single measurement vector (SMV) $\mathbf{x}(t) = [x_1(t), \ldots, x_M(t)]^{\mathrm{T}} \in \mathbb{C}^M$ at time instant t can be formulated as

$$\mathbf{x}(t) = \mathbf{A}\mathbf{s}(t) + \mathbf{n}(t). \tag{2}$$

It can be extended to multiple snapshots or multiple measurement vectors (MMV) $\mathbf{x}(t_n)$ at N time instants t_n, $n = 1, 2, \ldots, N$:

$$\mathbf{X} = \mathbf{A}\mathbf{S} + \mathbf{N} \tag{3}$$

with the matrix of measurements $\mathbf{X} = [\mathbf{x}(t_1), \ldots, \mathbf{x}(t_N)] \in \mathbb{C}^{M\times N}$, the signal matrix $\mathbf{S} = [\mathbf{s}(t_1), \ldots, \mathbf{s}(t_N)] \in \mathbb{C}^{K\times N}$ and the noise matrix $\mathbf{N} = [\mathbf{n}(t_1), \ldots, \mathbf{n}(t_N)] \in \mathbb{C}^{M\times N}$.

III. DoA Estimation

This section describes how the parameters of the measurement model (3), i.e., the spatial frequencies μ_k, and thus the DoAs θ_k of the K sources can be estimated for given measurements $\mathbf{X}$ by using the subspace-based methods MUSIC and ESPRIT as well as the CS-based methods BPDN and IHT.

A. Subspace-based Methods

The Subspace-based methods use the subspaces of the covariance matrix

$$\mathbf{R}_{\mathbf{xx}} = \mathrm{E}\left[\mathbf{x}(t)\, \mathbf{x}^{\mathrm{H}}(t)\right] \in \mathbb{C}^{M\times M} \tag{4}$$

of the measurements $\mathbf{x}(t)$ for estimating the DoAs. Orthonormal bases $\mathbf{U}_s \in \mathbb{C}^{M\times K}$ for the signal subspace and $\mathbf{U}_0 \in \mathbb{C}^{M\times(M-K)}$ for the noise subspace can be obtained by computing the EVD

$$\mathbf{R}_{\mathbf{xx}} = \mathbf{U}\mathbf{\Lambda}\mathbf{U}^{\mathrm{H}} \tag{5}$$

of $\mathbf{R}_{\mathbf{xx}}$, where $\mathbf{\Lambda} \in \mathbb{R}^{M\times M}$ is the diagonal matrix containing the eigenvalues in descending order and $\mathbf{U} = \begin{bmatrix}\mathbf{U_s} & \mathbf{U_0}\end{bmatrix} \in \mathbb{C}^{M\times M}$ a unitary matrix containing the eigenvectors. Since only N snapshots $\mathbf{X}$ are available, the covariance matrix $\mathbf{R}_{\mathbf{xx}}$ has to be estimated by

$$\hat{\mathbf{R}}_{\mathbf{xx}} = \frac{1}{N}\mathbf{X}\mathbf{X}^{\mathrm{H}}. \tag{6}$$

1) MUSIC: The MUSIC spectrum reads [2]

$$S(\mu) = \frac{1}{\mathbf{a}^{\mathrm{H}}(\mu)\, \mathbf{U_0}\mathbf{U_0}^{\mathrm{H}}\mathbf{a}(\mu)} \tag{7}$$

and is evaluated on a sampling grid $\{\theta_1, \theta_2, \ldots, \theta_P\}$ of P potential DoAs θ_i corresponding to the spatial frequencies $\mu_i = -\pi\sin(\theta_i)$, $i = 1, 2, \ldots, P$. The indices $l_k, k = 1, 2, \ldots, K$, of the spatial frequencies μ_{l_k} at which the K largest peaks of $S(\mu_i)$ occur finally determine the estimates $\hat{\theta}_k = \theta_{l_k}$ for the true DoAs of the K sources.

2) ESPRIT: If ESPRIT described in [3] is applied to a M-element ULA, which is considered as two subarrays consisting of the first and the last $M-1$ elements, the invariance equation

$$\mathbf{J}_1\mathbf{U}_s\mathbf{\Psi} = \mathbf{J}_2\mathbf{U}_s \tag{8}$$

has to be solved for $\mathbf{\Psi} \in \mathbb{C}^{K\times K}$ in a Least Squares (LS) sense. Here, $\mathbf{J}_1 = \left[\mathbf{1}_{M-1}, \mathbf{0}_{(M-1)\times 1}\right] \in \{0,1\}^{(M-1)\times M}$ and $\mathbf{J}_2 = \left[\mathbf{0}_{(M-1)\times 1}, \mathbf{1}_{M-1}\right] \in \{0,1\}^{(M-1)\times M}$ are selection matrices with the $(M-1)\times(M-1)$ identity matrix $\mathbf{1}_{M-1}$ and the zero vector $\mathbf{0}_{(M-1)\times 1}$ of length $M-1$. After computing the eigenvalues $\phi_k, k = 1, 2, \ldots, K$, of $\mathbf{\Psi}$, the estimates for the true DoAs of the K sources can be obtained as

$$\hat{\theta}_k = -\arcsin\left(\frac{\arg(\phi_k)}{\pi}\right). \tag{9}$$

B. Compressed Sensing (CS)-based Methods

CS aims at solving sparse recovery problems [4]. In the SMV case, a signal vector $\mathbf{s} \in \mathbb{C}^P$ that is K-sparse, i.e., has at most $K \ll P$ non-zero entries, is to be recovered from $M < P$ linear measurements $\mathbf{x} = \mathbf{A}\mathbf{s} \in \mathbb{C}^M$ taken by the measurement matrix $\mathbf{A} \in \mathbb{C}^{M\times P}$. The support of the vector $\mathbf{s} = [s_1, \ldots, s_P]^{\mathrm{T}}$ is defined as the index set $\mathrm{supp}(\mathbf{s}) = \{i : s_i \neq 0\}$ of its non-zero entries. The so-called ℓ_0 "norm" $\|\mathbf{s}\|_0 = |\mathrm{supp}(\mathbf{s})|$ of the vector $\mathbf{s}$ counts its non-zero elements. In the MMV case, a signal matrix $\mathbf{S} = [\mathbf{s}_1, \ldots, \mathbf{s}_N] \in \mathbb{C}^{P\times N}$ that consists of N jointly K-sparse signal vectors $\mathbf{s}_n$, $n = 1, 2, \ldots, N$, with the same support and is therefore row K-sparse, i.e., has at most $K \ll P$ non-zero rows, is to be recovered from the matrix $\mathbf{X} = [\mathbf{x}_1, \ldots, \mathbf{x}_N] = \mathbf{A}\mathbf{S} \in \mathbb{C}^{M\times N}$ consisting of N measurement vectors $\mathbf{x}_n$. The number of non-zero rows of $\mathbf{S}$ can be expressed as $\|\mathbf{S}\|_{p,0}$. The mixed $\ell_{p,q}$ norm of $\mathbf{S}$ with rows $\mathbf{s}^i$, $i = 1, 2, \ldots, P$, is defined as

$$\|\mathbf{S}\|_{p,q} = \left\| \left[\|\mathbf{s}^1\|_p, \|\mathbf{s}^2\|_p, \ldots, \|\mathbf{s}^P\|_p \right] \right\|_q. \tag{10}$$

Furthermore, CS deals with the recovery of sparse signals from measurements contaminated by noise, which makes the CS framework applicable to the DoA estimation.

Up to now, the signal matrix $\mathbf{S}$ in the measurement model (3) is not row K-sparse. In order to make it row K-sparse, the angle $\theta \in [-90°, 90°)$ is discretized similarly to [5], which results in a sampling grid $\{\theta_1, \theta_2, \ldots, \theta_P\}$ of $P \gg K$ potential DoAs θ_i corresponding to the spatial frequencies $\mu_i = -\pi\sin(\theta_i)$, $i = 1, 2, \ldots, P$. Let $\mathcal{I} = \{i_1, i_2, \ldots, i_K\} \subset \{1, 2, \ldots, P\}$ be an ordered set of indices

ISBN 978-3-8007-3662-1

i_k indicating that the k^{th} source is located at the grid point i_k. The array steering matrix $\mathbf{A} = [\mathbf{a}(\mu_{i_1}), \ldots, \mathbf{a}(\mu_{i_K})] \in \mathbb{C}^{M \times K}$ of the measurement model (3), whose k^{th} column $\mathbf{a}(\mu_{i_k})$ corresponds to the k^{th} source, is extended to the array steering matrix $\mathbf{A} = [\mathbf{a}(\mu_1), \ldots, \mathbf{a}(\mu_P)] \in \mathbb{C}^{M \times P}$, whose i^{th} column $\mathbf{a}(\mu_i)$ corresponds to the direction θ_i of the sampling grid. The signal vectors $\mathbf{s}(t_n)$ in the signal matrix $\mathbf{S}$ of the measurement model (3) are extended from $\mathbf{s}(t) = [s_{i_1}(t), \ldots, s_{i_K}(t)]^{\mathrm{T}} \in \mathbb{C}^K$, whose k^{th} element $s_{i_k}(t)$ is the signal from source k, to $\mathbf{s}(t) = [s_1(t), \ldots, s_P(t)]^{\mathrm{T}} \in \mathbb{C}^P$, whose i^{th} element $s_i(t)$ is the signal from the direction θ_i of the sampling grid. Since

$$s_i(t) = \begin{cases} s_{i_k}(t), & i = i_k \in \mathcal{I} \\ 0, & \text{otherwise} \end{cases}, i = 1, 2, \ldots, P,$$

and thus $s_i(t)$ is only non-zero if one of the K sources is located at grid point i, the signal vectors $\mathbf{s}(t_n)$ are jointly K-sparse with $\operatorname{supp}(\mathbf{s}(t_n)) = \mathcal{I}$ and the signal matrix $\mathbf{S}$ is row K-sparse. The DoA estimation can be considered as the sparse recovery problem of obtaining a row K-sparse estimate $\hat{\mathbf{S}} = [\hat{\mathbf{s}}(t_1), \ldots, \hat{\mathbf{s}}(t_N)]$ for the true row K-sparse signal matrix $\mathbf{S}$ from the measurements $\mathbf{X}$ with the array steering matrix $\mathbf{A}$ as the measurement matrix. The indices of the non-zero rows of $\hat{\mathbf{S}}$, i.e., $\operatorname{supp}(\hat{\mathbf{s}}(t_n)) = \{l_1, l_2, \ldots, l_K\}$, finally determine the estimates $\hat{\theta}_k = \theta_{l_k}$ for the true DoAs of the K sources.

After formulating the DoA estimation as a sparse recovery problem, it can be solved by methods of CS.

1) BPDN: The row K-sparse signal matrix $\mathbf{S}$ can be recovered by using BPDN [8]:

$$\hat{\mathbf{S}} = \underset{\tilde{\mathbf{S}} \in \mathbb{C}^{P \times N}}{\operatorname{argmin}} \left\| \tilde{\mathbf{S}} \right\|_{2,1} \quad \text{s.t.} \quad \left\| \mathbf{A}\tilde{\mathbf{S}} - \mathbf{X} \right\|_F \leq \beta. \tag{11}$$

The objective of the optimization problem ensures that the estimate $\hat{\mathbf{S}}$ is row sparse while its constraint forces it to be consistent with the measurements $\mathbf{X}$. The regularization parameter β has to be chosen appropriately depending on the noise, which is the main drawback of this approach.

2) IHT: The greedy IHT algorithm described in [4] and [9] tries to solve the optimization problem

$$\hat{\mathbf{s}} = \underset{\tilde{\mathbf{s}} \in \mathbb{C}^P}{\operatorname{argmin}} \left\| \mathbf{A}\tilde{\mathbf{s}} - \mathbf{x} \right\|_2^2 \quad \text{s.t.} \quad \left\| \tilde{\mathbf{s}} \right\|_0 \leq K \tag{12}$$

iteratively in order to recover the K-sparse signal vector $\mathbf{s} \in \mathbb{C}^P$ from a SMV $\mathbf{x} = \mathbf{A}\mathbf{s} + \mathbf{n} \in \mathbb{C}^M$ of measurements taken by the measurement matrix $\mathbf{A} \in \mathbb{C}^{M \times P}$ and contaminated by noise $\mathbf{n} \in \mathbb{C}^M$. Compared to BPDN, the roles of the objective and the constraint are exchanged. Now, the constraint ensures that the estimate $\hat{\mathbf{s}}$ is K-sparse while the objective forces it to be consistent with the measurements $\mathbf{x}$.

Each iteration of IHT consists of two steps, a gradient descent step and a hard thresholding step. The gradient descent step

$$\check{\mathbf{s}}^{(i+1)} = \hat{\mathbf{s}}^{(i)} + \mu \mathbf{A}^{\mathrm{H}} \left(\mathbf{x} - \mathbf{A}\hat{\mathbf{s}}^{(i)} \right) \tag{13}$$

with step size μ starting at the current estimate $\hat{\mathbf{s}}^{(i)}$ reduces the consistency-enforcing objective. The hard thresholding step ensures that the constraint is fulfilled by applying the hard thresholding operator $H_K(.)$, which sets all but the K largest in magnitude elements to 0, to the resulting vector $\check{\mathbf{s}}^{(i+1)}$ to get a new K-sparse estimate $\hat{\mathbf{s}}^{(i+1)} = H_K\left(\check{\mathbf{s}}^{(i+1)}\right)$.

In order to recover the row K-sparse signal matrix $\mathbf{S} \in \mathbb{C}^{P \times N}$ from the MMV $\mathbf{X} \in \mathbb{C}^{M \times N}$ according to the measurement model (3), we would like to solve the optimization problem

$$\hat{\mathbf{S}} = \underset{\tilde{\mathbf{S}} \in \mathbb{C}^{P \times N}}{\operatorname{argmin}} \left\| \mathbf{A}\tilde{\mathbf{S}} - \mathbf{X} \right\|_F^2 \quad \text{s.t.} \quad \left\| \tilde{\mathbf{S}} \right\|_{p,0} \leq K. \tag{14}$$

The constraint ensures that the estimate $\hat{\mathbf{S}}$ is row K-sparse whereas the objective forces it to be consistent with the measurements $\mathbf{X}$.

The standard IHT algorithm for the SMV case has to be modified to solve the new optimization problem of the MMV scenario. In each iteration, the value of the new consistency-enforcing objective is reduced by computing the gradient descent step

$$\check{\mathbf{S}}^{(i+1)} = \hat{\mathbf{S}}^{(i)} + \mu \mathbf{A}^{\mathrm{H}} \left(\mathbf{X} - \mathbf{A}\hat{\mathbf{S}}^{(i)} \right) \tag{15}$$

starting at the current estimate $\hat{\mathbf{S}}^{(i)}$ simultaneously for all MMV according to (13) with step size μ. Applying the hard thresholding operator $\bar{H}_K(.)$ to the resulting matrix $\check{\mathbf{S}}^{(i+1)}$ sets all but the K rows with the largest ℓ_2 norm to $\mathbf{0}^{\mathrm{T}}$ to get a new row K-sparse estimate $\hat{\mathbf{S}}^{(i+1)} = \bar{H}_K\left(\check{\mathbf{S}}^{(i+1)}\right)$, which ensures that the constraint is fulfilled.

The resulting IHT algorithm for the MMV scenario is described in Algorithm 1.

Algorithm 1 IHT for MMV

Input: $\mathbf{X}$, $\mathbf{A}$, K, μ
  Initialize: $\hat{\mathbf{S}}^{(0)} = \mathbf{0}$, $i = 0$
  while stopping criterion not met **do**
    $\hat{\mathbf{S}}^{(i+1)} = \bar{H}_K\left(\hat{\mathbf{S}}^{(i)} + \mu \mathbf{A}^{\mathrm{H}}\left(\mathbf{X} - \mathbf{A}\hat{\mathbf{S}}^{(i)}\right)\right)$
    $i := i + 1$
  end while
Output: $\hat{\mathbf{S}}^{(i)}$

IV. DoA Estimation Performance

We examined the DoA estimation performance of the subspace-based methods MUSIC and ESPRIT as well as the one of the CS-based methods BPDN and IHT for small- and large-scale antenna arrays in simulations. The results of the simulations are presented in this section.

The DoA estimation performance is measured in terms of the root mean square error (RMSE)

$$\text{RMSE}_\theta = \sqrt{\frac{1}{RK} \sum_{r=1}^{R} \sum_{k=1}^{K} \left| \hat{\theta}_{k,r} - \theta_k \right|^2} \tag{16}$$

between the DoAs θ_k of the sources $k = 1, 2, \ldots, K$ and their estimates $\hat{\theta}_{k,r}$ in $R = 100$ Monte Carlo runs $r = 1, 2, \ldots, R$.

ISBN 978-3-8007-3662-1

The sampling grid used for MUSIC, BPDN and IHT is constructed from the $P = 1024$ angles $\theta_i = \arcsin\left(\frac{2}{P}(i-1)-1\right)$ corresponding to the equally spaced spatial frequencies $\mu_i = \pi - \frac{2\pi}{P}(i-1)$, $i = 1, 2, \ldots, P$. Since the absolute inner product between neighboring columns of $\mathbf{A}$ is pretty high for a large P, we decided to let the hard thresholding operator $\bar{H}_K(.)$ in IHT set all but the K rows at which the ℓ_2 norm of the rows has its largest peaks to $\mathbf{0}^{\mathrm{T}}$. $\bar{H}_K(.)$ is also applied to the estimate of BPDN to make it row K-sparse if it has more than K non-zero rows.

$K = 2$ sources are located at the angles $\theta_1 = 4.93°$ and $\theta_2 = 10.01°$. They are uncorrelated and emit equipower QPSK-symbols with zero mean and variance $\sigma_s^2 = 1$, whereas the measurement noise samples are drawn from an i.i.d. circularly symmetric complex Gaussian random process with zero mean and variance σ_n^2. The SNR in dB is defined as

$$\mathrm{SNR} = 10\log_{10}\left(\frac{K\sigma_s^2}{\sigma_n^2}\right)\ \mathrm{dB} \tag{17}$$

and chosen to be 10 dB for all simulations.

In order to reduce the computational complexity of BPDN, the matrix of measurements $\mathbf{X} \in \mathbb{C}^{M\times N}$ is compressed to the matrix $\mathbf{X}_{\mathrm{SVD}} \in \mathbb{C}^{M\times K}$ used in BPDN instead of $\mathbf{X}$ by the ℓ_1-SVD described in [5] if the number of snapshots is larger than the number of sources, i.e., $N > K$. As mentioned previously, the appropriate choice of the regularization parameter β in (11) is important. For the simulations, we chose it to be

$$\beta = \sqrt{\min(K, N)\, M\sigma_n^2}. \tag{18}$$

In addition to the RMSE of the considered DoA estimation methods, we also provide the Cramér-Rao Bound (CRB).

As can be seen in Fig. 1, for a small-scale antenna array with $M = 8$ antenna elements, the RMSE of IHT is larger than $10°$ regardless of the number of snapshots N. BPDN performs better than IHT and achieves a RMSE of approximately $1°$ if enough snapshots are available. If the number of snapshots is sufficiently large, the two subspace-based methods MUSIC and ESPRIT exhibit a similar performance that is much better than the one of the CS-based methods.

On the contrary, ESPRIT shows the worst performance of all methods regardless of the number of snapshots N if a large-scale antenna array with $M = 64$ antenna elements is used for DoA estimation, as the simulation results in Fig. 2 demonstrate. If the number of snapshots is small, MUSIC and the CS-based methods perform significantly better than ESPRIT. They are even able to estimate the DoAs with only one single snapshot and a very small RMSE. While the RMSE of MUSIC and IHT is almost identical for one snapshot, the performance gap between both algorithms increases with increasing number of snapshots since MUSIC can exploit the availability of more snapshots better than IHT. The smallest RMSE of all methods regardless of the number of snapshots is achieved by BPDN.

In Fig. 3 the RMSE is plotted over the number of antenna elements M for $N = 100$ snapshots. If a large number of snapshots as in this case is available, a small number of

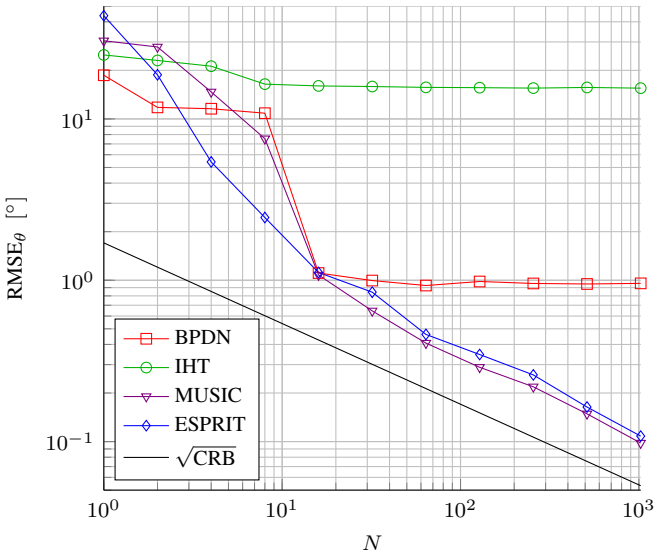

Fig. 1. RMSE$_\theta$ vs. N for $M = 8$.

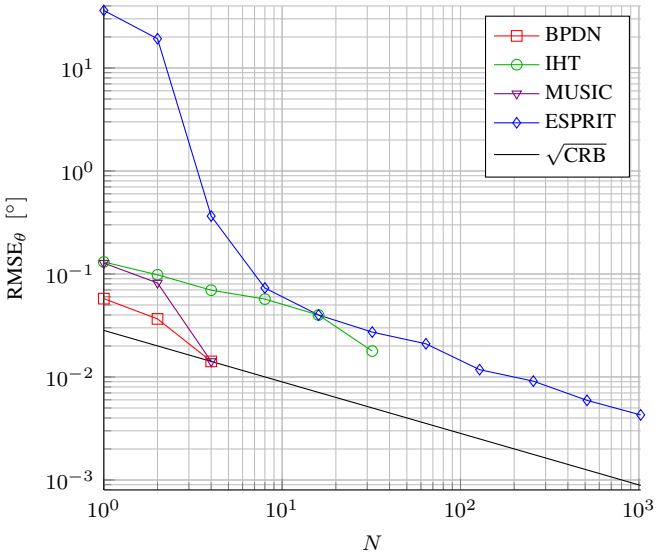

Fig. 2. RMSE$_\theta$ vs. N for $M = 64$.

antenna elements is sufficient for ESPRIT to estimate the DoAs with a RMSE that is smaller than the one of all other methods. They require more antenna elements to achieve the same performance as ESPRIT. For a small number of antenna elements, BPDN and IHT perform better than MUSIC, which, however, becomes better than BPDN and IHT with increasing number of antenna elements. The RMSE curve of BPDN always lies below the one of IHT.

If only $N = 2$ snapshots are available, ESPRIT is not able to estimate the DoAs any more and increasing the number of antenna elements cannot compensate for the small number of snapshots, which becomes apparent in Fig. 4. The performance of IHT and MUSIC is comparable and both outperform ESPRIT for a large number of antenna elements since their DoA estimation performance improves significantly

ISBN 978-3-8007-3662-1

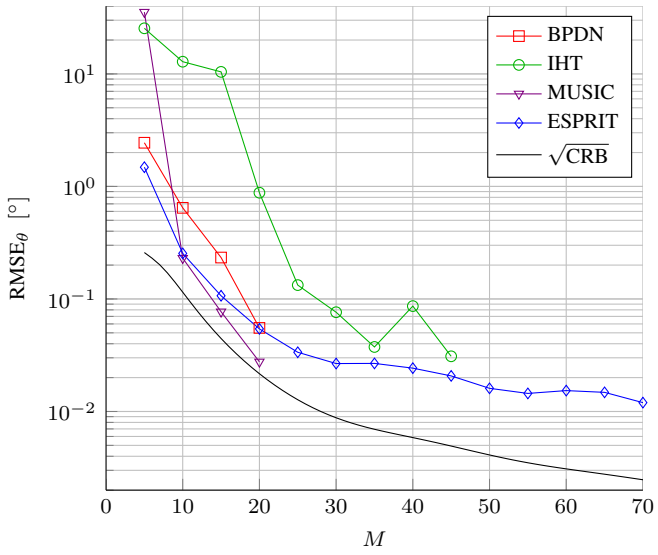

Fig. 3. RMSE_θ vs. M for $N = 100$.

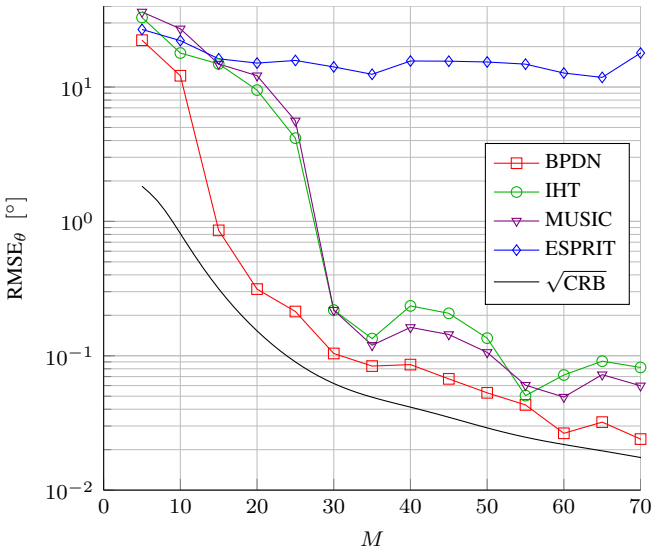

Fig. 4. RMSE_θ vs. M for $N = 2$.

with increasing number of antenna elements. Only BPDN is able to provide even better DoA estimates. The large performance gap between the two subspace-based methods MUSIC and ESPRIT is due to the fact that MUSIC works on the noise subspace whereas ESPRIT works on the signal subspace. The dimension of the noise subspace is $M - K$ and thus grows with increasing number of antenna elements M. The dimension of the signal subspace, however, is K and thus independent of the number of antenna elements M. If the number of antenna elements M is very large compared to the number of sources K, the dimension of the noise subspace is very large such that the estimation of the noise subspace from a small number of snapshots is more robust than the one of the signal subspace with the relatively small dimension K. This explains why MUSIC is able to perform much better than ESPRIT in this scenario.

A similar picture emerges if the measurements at the antenna elements are additionally quantized to 1 bit such that only the signs of the real and imaginary parts of the measurements can be used for DoA estimation. For a small number of antenna elements and a large number of snapshots, ESPRIT has a better DoA estimation performance than the other methods (see Fig. 5). For a large number of antenna elements and a small number of snapshots, IHT is competitive to BPDN[1] and MUSIC, which outperform ESPRIT (see Fig. 6). This result is of interest especially in massive MIMO systems, where the number of antenna elements is very large and 1-bit quantization is used in order to reduce the complexity, power consumption and costs resulting from the large number of antenna elements.

[1]Please note that the regularization parameter β has to be adapted to the case of 1-bit quantization, e.g., by choosing $\beta = \sqrt{1.5 \min(K, N) M (\sigma_n^2 + 3^{-1})}$.

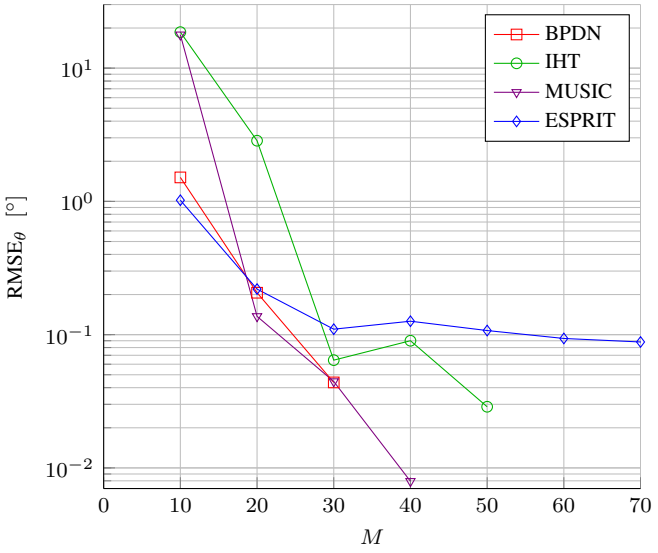

Fig. 5. RMSE_θ vs. M for $N = 100$ and 1-bit quantization.

V. Computational Complexity

In practical applications, not only the DoA estimation performance of the methods is important but also their computational complexity. Therefore, we compare the computational complexity of the subspace-based methods MUSIC and ESPRIT as well as the one of the CS-based methods BPDN and IHT in this section.

If the matrix of measurements is compressed by the ℓ_1-SVD, the DoAs can be estimated using BPDN with a computational complexity of $\mathcal{O}\left(K^3 P^3\right)$ [5]. This is larger than the costs of the subspace-based methods MUSIC and ESPRIT, which are $\mathcal{O}\left(M^2 P + M^2 N\right)$ and $\mathcal{O}\left(M^3 + M^2 N\right)$, respectively. MUSIC is computationally more complex than ESPRIT due to the spectral search, i.e., the evaluation of (7) on the sampling grid of $P > M$ spatial frequencies. The computational com-

ISBN 978-3-8007-3662-1

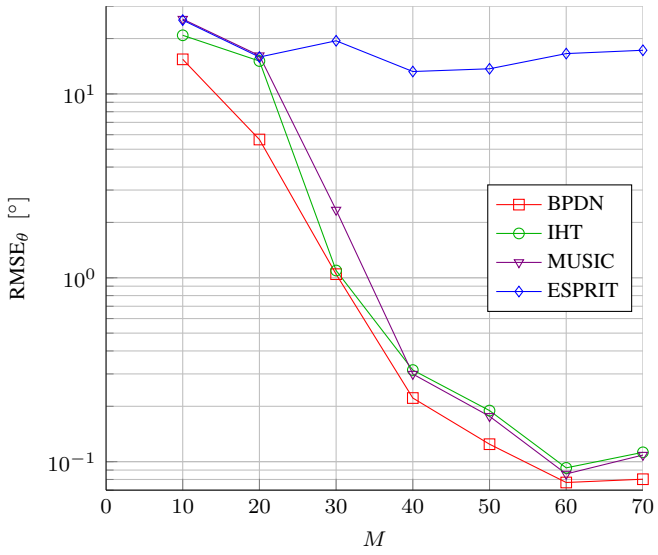

Fig. 6. RMSE$_\theta$ vs. M for $N = 2$ and 1-bit quantization.

TABLE I
COMPUTATIONAL COMPLEXITY OF BPDN, IHT, MUSIC AND ESPRIT.

BPDN	$\mathcal{O}\left(K^3P^3\right)$
IHT	$\mathcal{O}\left(MNP\right)$ (per iteration)
MUSIC	$\mathcal{O}\left(M^2P + M^2N\right)$
ESPRIT	$\mathcal{O}\left(M^3 + M^2N\right)$

plexity of ESPRIT is dominated by the subspace estimation using the EVD of the covariance matrix. Each iteration of IHT consists only of matrix additions and multiplications as well as the thresholding operation, whose cost is $\mathcal{O}\left(MNP\right)$. Empirically, we found out that a few iterations are sufficient for DoA estimation. In the extreme case, only one iteration is necessary. If the number of snapshots N is small and the number of antenna elements M becomes very large, the subspace estimation using the EVD of the covariance matrix with a cost of $\mathcal{O}\left(M^3\right)$ for the subspace-based methods and the spectral search of MUSIC with a cost of $\mathcal{O}\left(M^2P\right)$ become computationally intractable such that the computational complexity of IHT is smaller than the one of the subspace-based methods. Tab. I lists the computational complexity of all considered methods.

From this comparison of the computational complexity of the DoA estimation methods, we can conclude that ESPRIT is the method of choice for a scenario with a small number of antenna elements and a large number of snapshots. In this situation, it combines the smallest computational complexity and a good DoA estimation performance. In a scenario, where many antenna elements but only a few snapshots are available, however, IHT having the smallest computational complexity of all methods achieves a DoA estimation performance that is almost as good as the one of BPDN and MUSIC, and much better than the one of ESPRIT.

VI. CONCLUSION

In this paper, we compared the subspace-based methods MUSIC and ESPRIT as well as the CS-based methods BPDN and IHT for DoA estimation in terms of both DoA estimation performance and computational complexity for small- and large-scale antenna arrays. After introducing the measurement model for DoA estimation with the help of a ULA, we described how the DoAs can be estimated using the four considered methods MUSIC, ESPRIT, BPDN and IHT. The simulation results reveal that the subspace-based methods in general and ESPRIT in particular achieve a smaller RMSE in the DoAs and thus a better DoA estimation performance than the CS-based methods if a small-scale antenna array with a small number of antenna elements is used and a large number of snapshots is available. For a large-scale antenna array with a large number of antenna elements, the CS-based methods perform equally well as or even better than the subspace-based methods especially if the number of available snapshots is small. The comparison of the computational complexity shows that the EVD of the covariance matrix for the subspace-based methods becomes computationally intractable for large-scale antenna systems such that the computational complexity of IHT is smaller than the one of the subspace-based methods. Therefore, it can be concluded that the subspace-based method ESPRIT is well suited for scenarios with a small-scale antenna array and many snapshots whereas IHT is advantageous for scenarios with a large-scale antenna array and only a few snapshots as in massive MIMO, a potential candidate for the future generation of wireless communication systems.

REFERENCES

[1] Nokia Solutions and Networks, "Technology Vision 2020," White Paper, June 2013.
[2] R. Schmidt, "Multiple emitter location and signal parameter estimation," *Antennas and Propagation, IEEE Transactions on*, vol. 34, no. 3, pp. 276–280, Mar 1986.
[3] A. Paulraj, R. Roy, and T. Kailath, "Estimation of signal parameters via rotational invariance techniques- Esprit," in *Circuits, Systems and Computers, 1985. Nineteeth Asilomar Conference on*, Nov 1985, pp. 83–89.
[4] Y. C. Eldar and G. Kutyniok, *Compressed Sensing Theory and Applications*. Cambridge Univ. Press, 2012.
[5] D. Malioutov, M. Cetin, and A. Willsky, "A sparse signal reconstruction perspective for source localization with sensor arrays," *Signal Processing, IEEE Transactions on*, vol. 53, no. 8, pp. 3010–3022, Aug 2005.
[6] L. Carin, D. Liu, and B. Guo, "Coherence, compressive sensing, and random sensor arrays," *Antennas and Propagation Magazine, IEEE*, vol. 53, no. 4, pp. 28–39, Aug 2011.
[7] C. Svensson, S. Andersson, and P. Bogner, "On the power consumption of analog to digital converters," in *Norchip Conference, 2006. 24th*, Nov 2006, pp. 49–52.
[8] E. van den Berg and M. P. Friedlander, "Sparse optimization with least-squares constraints," *SIAM J. Optimization*, vol. 21, no. 4, pp. 1201–1229, 2011.
[9] T. Blumensath and M. E. Davies, "Iterative hard thresholding for compressed sensing," *CoRR*, vol. abs/0805.0510, 2008.

ISBN 978-3-8007-3662-1